ACS Sustainable Chemistry & Engineering

Research Article

pubs.acs.org/journal/ascecg

Shape- and Morphology-Controlled Sustainable Synthesis of Cu, Co, and In Metal Organic Frameworks with High CO_2 Capture Capacity

Pradip Sarawade, Hua Tan, and Vivek Polshettiwar*

Nanocatalysis Laboratory (NanoCat), KAUST Catalysis Center (KCC), King Abdullah University of Science and Technology (KAUST), Thuwal 23955, KSA

Supporting Information

ABSTRACT: We studied the effects of various surfactants on the shape and morphology of three metal organic frameworks (MOFs), i.e., Co-MOF, Cu-MOF, and In-MOF, which were synthesized under microwave irradiation. The as-synthesized materials were characterized by X-ray powder diffraction (XRD), scanning electron microscopy (SEM), thermogravimetric analysis (TGA), and nitrogen sorption. The effects of microwave irradiation time, temperature, and surfactant template were investigated. The synthetic parameters, including the type of surfactant template and the reaction temperature, played crucial roles in the size, shape, and morphology of the MOF microcrystals. We also evaluated these MOFs as sorbents for capturing CO_2. Of the synthesized materials, Cu-MOF demonstrated the highest CO_2 capture capacity, even at atmospheric pressure and ambient temperature.

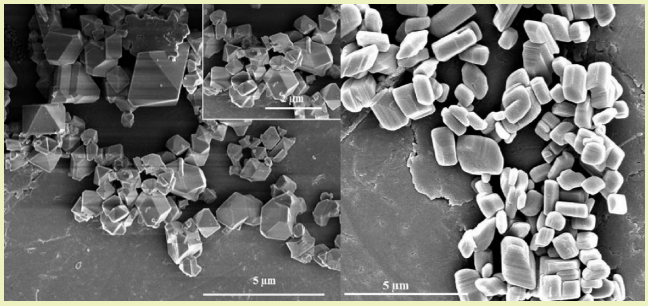

KEYWORDS: *Metal organic frameworks, shape, morphology, microwave, CO_2 capture capacity*

INTRODUCTION

Materials with high porosity and low density have attracted significant attention recently because they offer the combined advantages of high surface area, high pore volume, and larger pore size. In recent years, metal−organic frameworks (MOFs) have emerged as a new class of hybrid, highly nanoporous crystalline materials with extremely high porosity.[1−9] MOFs also possess tailorable molecular cavities, adjustable functionality, and extremely large surface area. They have been shown to have potential applications in gas storage and separation,[10] catalysis,[11] drug delivery,[8,12,13] and CO_2 capture.[14−16]

The surfactant-templating method has been widely used to control the size and shape of metals and metal oxides.[17,18] Recently, it was observed that surfactant templates can play a decisive role in the preparation of mesoporous MOFs.[19−26] The surfactant, which acts as a capping reagent during the synthetic process, can decrease the surface energy and total system energy via dipole−dipole interactions or van der Waals forces that can control the crystal growth and facilitate the formation of various morphologies. Despite the continuous progress in this field, a rapid, shape-controlled synthetic method for fabricating MOFs remains unavailable. Therefore, a sustainable and effective shape-controlled synthetic route to MOFs is highly desirable.

As a continuation of our work on shape- and morphology-controlled nanomaterial synthesis and catalysis[27−35] and a step toward the development of novel CO_2 sorbents,[32] we report the synthesis of MOFs with various shapes and morphologies along with their application as sorbents for capturing CO_2 at atmospheric pressure. Three surfactants as structure-directing agents, i.e., cetyltrimethylammonium bromide (CTAB), sodium dodecyl sulfate (SDS), and pluronic triblock copolymer (P-123), were used to construct Co-MOF, Cu-MOF, and In-MOF. We used ligands bipyen (*trans*-1,2-bis(4-pyridyl)ethylene); ndc (2,6-naphthalenedicarboxylic acid) for Co-MOF; BTC (1,3,5-benzenetricarboxylic acid) for Cu-MOF; and Himdc (4,5-imidazoledicarboxylate), H_2dach (4,5-imidazoledicarboxylic), and DMF (*N*,*N*-dimethylformamide) for In-MOF. We obtained different shapes and morphologies for these MOF microcrystals depending on the reaction conditions and template used (Figure 1).

EXPERIMENTAL SECTION

Synthesis of Co-MOF. In a typical synthesis, the template (CTAB, SDS, and P123) (0.5 g) was dissolved in water (25 mL) and stirred for 30 min. A mixture of $Co(NO_3)2.6\ H_2O$ (0.32 g), H_2ndc (0.24 g), and bipyen (0.20 g) in a molar ratio of 1:1:1 was stirred in an additional 25 mL of water for 30 min at room temperature. This mixture was then added to the first solution with continuous stirring for 30 min. The reaction solution was then transferred to a 60-mL Teflon-sealed microwave reactor. The reaction mixture was exposed to microwave (MW) radiation (800 W maximum power) at 180 °C for 4 h. To determine the growth mechanism of the MOF crystals, we conducted a series of experiments with varying reaction temperatures and times. After the reaction mixture cooled to room temperature, the product was isolated by centrifugation and washed thoroughly thrice with water, thrice with ethanol, and once with acetone prior to air drying at

Received: July 8, 2012
Revised: October 15, 2012
Published: November 6, 2012

   dx.doi.org/10.1021/sc300036p | *ACS Sustainable Chem. Eng.* 2013, 1, 66−74

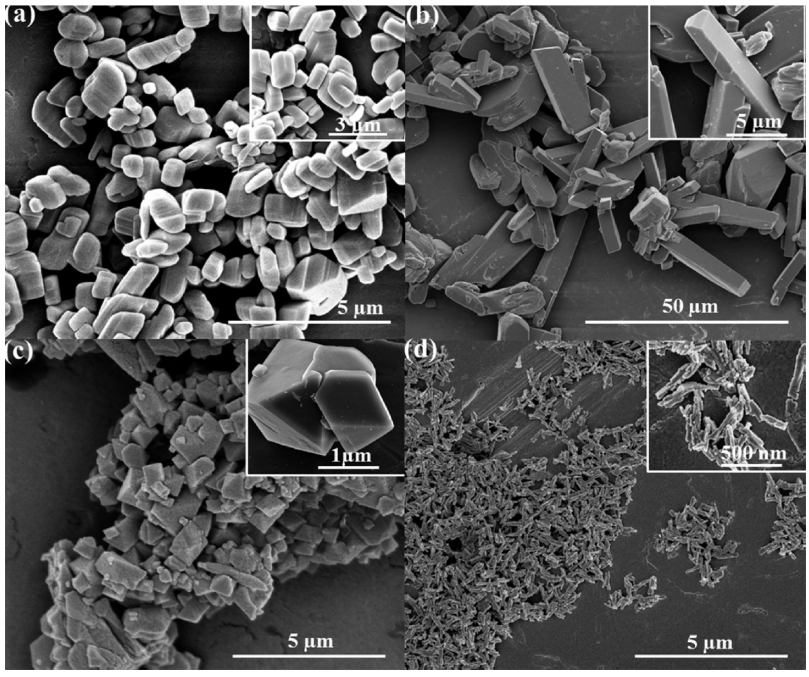

Figure 1. SEM images of the as-synthesized MOF microcrystals: (a and b) Co-MOF, (c) Cu-MOF, and (d) In-MOF. The images in the insets are close-up views of the various MOF microcrystals.

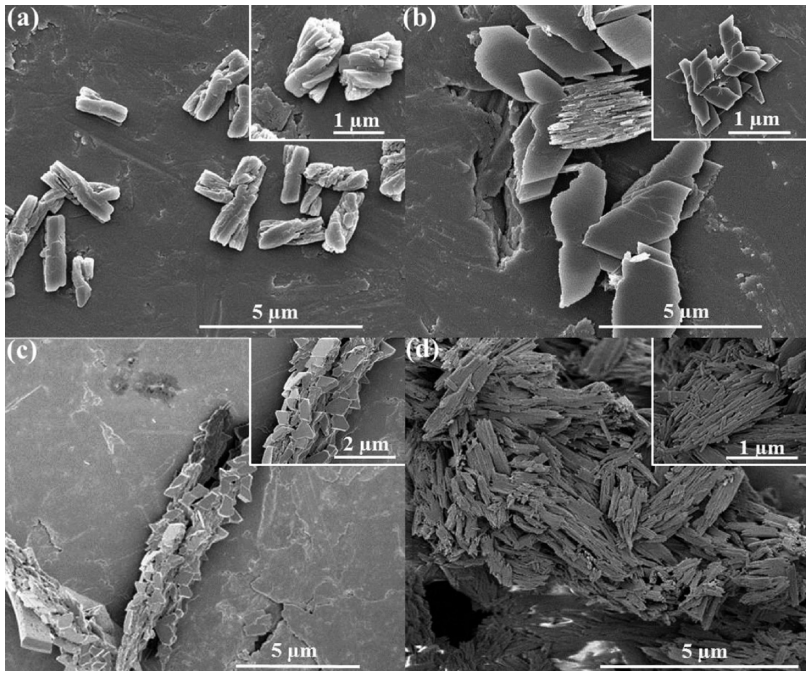

Figure 2. SEM images of as-synthesized Co-MOF microcrystals with and without a surfactant: (a) without a surfactant, (b) CTAB, (c) SDS, and (d) P123. The images in the insets are close-up views of the Co-MOF microcrystals. (MW at 120 °C for 0 min, ramp time 5 min.)

room temperature. To completely remove the surfactant from the pores, the product was refluxed in ethanol 6 times at 80 °C for 2 h.

Synthesis of Cu-MOF. To synthesize monodisperse Cu-MOF nanocrystals, 0.314 g of $Cu(NO_3)\cdot 3H_2O$ was dissolved in water (25 mL). BTC (0.1 M) in pure ethanol (13.3 mL) was added to this aqueous solution. The mixture was stirred for 30 min at room temperature, slowly added to the aqueous template solution, and then stirred for an additional 30 min at room temperature. The reaction solution was then transferred to a 60-mL Teflon-sealed microwave reactor. The reaction mixture was exposed to microwave (MW) radiation (800 W maximum power) at 120 °C for 4 h. The product was then collected using the procedure described above for microwave synthesis of the Co-MOF microcrystal.

Synthesis of In-MOF. To synthesize In-MOF nanocrystal rods, a mixture of 4,5-imidazoledicarboxylic acid (0.014 g, 0.087 mmol), $In(NO_3)_3\cdot 2H_2O$ (0.015 g, 0.0435 mmol), DMF (1 mL), CH_3CN (1 mL), 1,2-diaminocyclohexane (0.1 mL, 10.75 M in DMF), and HNO_3 (0.5 mL, 3.5 M in DMF) dissolved in water (25 mL) was stirred for 30 min prior to slow addition to the aqueous template solution and stirring for an additional 30 min at room temperature. The reaction solution was then transferred to a 60-mL Teflon-sealed MW reactor and exposed to microwave (MW) radiation (800 W maximum power)

dx.doi.org/10.1021/sc300036p | ACS Sustainable Chem. Eng. 2013, 1, 66−74

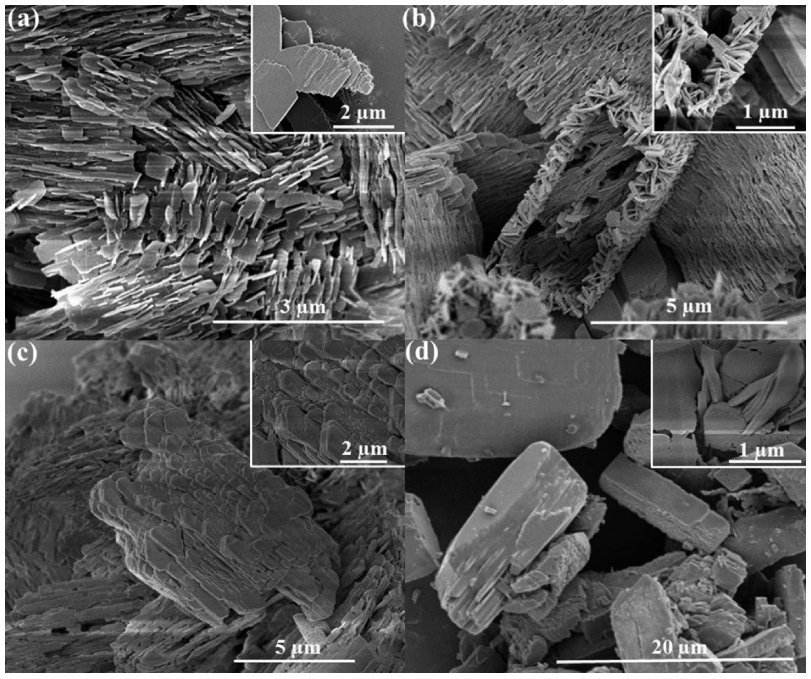

Figure 3. SEM images of as-synthesized Co-MOF microcrystals in the presence of the CTAB surfactant. (a) MW at 120 °C for 5 min with a ramp time of 5 min; (b) MW at 160 °C for 5 min with a ramp time of 30 min; (c) MW at 180 °C for 30 min with a ramp time of 30 min; and (d) MW at 180 °C for 4 h with a ramp time of 30 min. The insets show close-up views of Co-MOF microcrystals.

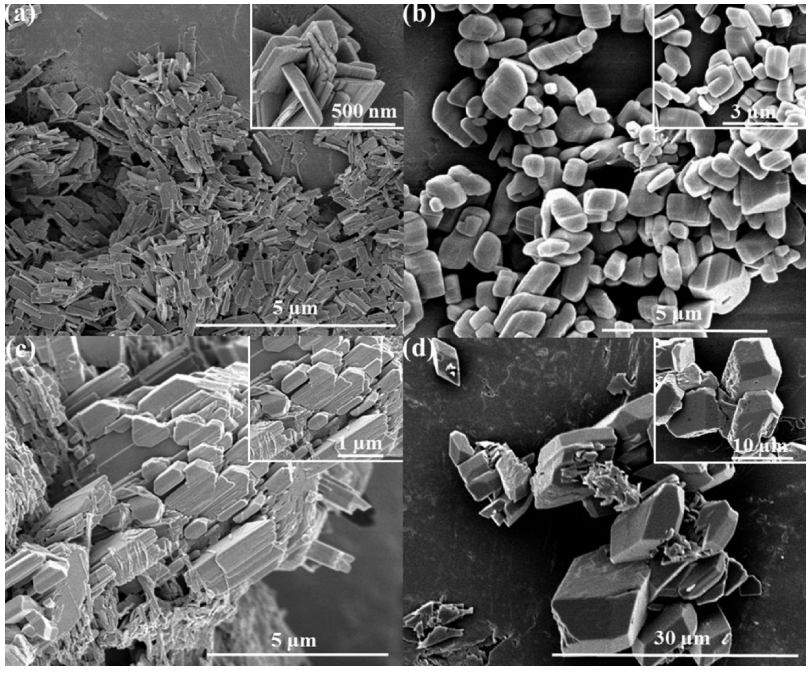

Figure 4. SEM images of as-synthesized Co-MOF microcrystals in the presence of SDS surfactant. (a) MW at 120 °C for 5 min, ramp time of 5 min; (b) MW at 160 °C for 5 min, ramp time of 30 min; (c) MW at 180 °C for 30 min, ramp time of 30 min; and (d) MW at 180 °C for 4 h, ramp time of 30. The images in the insets are close-up views of the Co-MOF microcrystals.

at 120 °C for 4 h. The product was then collected by using the same procedure described above for the microwave synthesis of Co-MOF microcrystals.

RESULTS AND DISCUSSION

It is well-established that microwave (MW) heating promotes rapid, uniform nucleation and crystallization in supersaturated substrate solutions via a molecular rotation heating mechanism.[33−35] We therefore used a MW-assisted synthesis to synthesize the MOFs. Microcrystals of various shapes and sizes were prepared by tuning both the reaction time and temperature in the presence of three different surfactants. Figure 1 shows the scanning electron microscopy (SEM) images of as-synthesized cobalt (Co), copper (Cu), and indium (In) MOFs with various shapes.

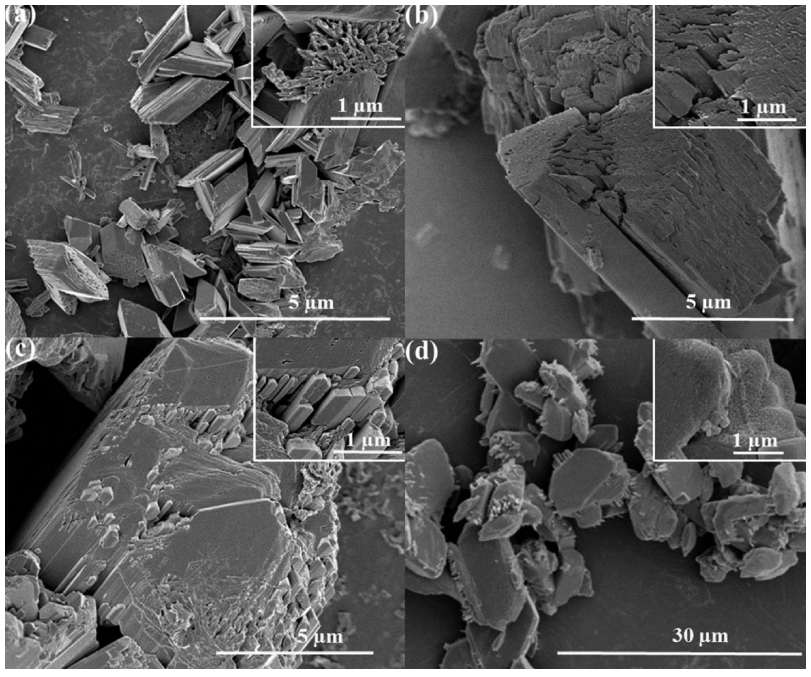

Figure 5. SEM images of as-synthesized Co-MOF microcrystals in the presence of P123 surfactant. (a) MW at 120 °C for 5 min, ramp time of 5 min; (b) MW at 160 °C for 5 of min, ramp time 30 min; (c) MW at 180 °C for 30 min, ramp time of 30 min; and (d) MW at 180 °C for 4 h, ramp time of 30 min. The images in the insets are close-up views of the Co-MOF microcrystals.

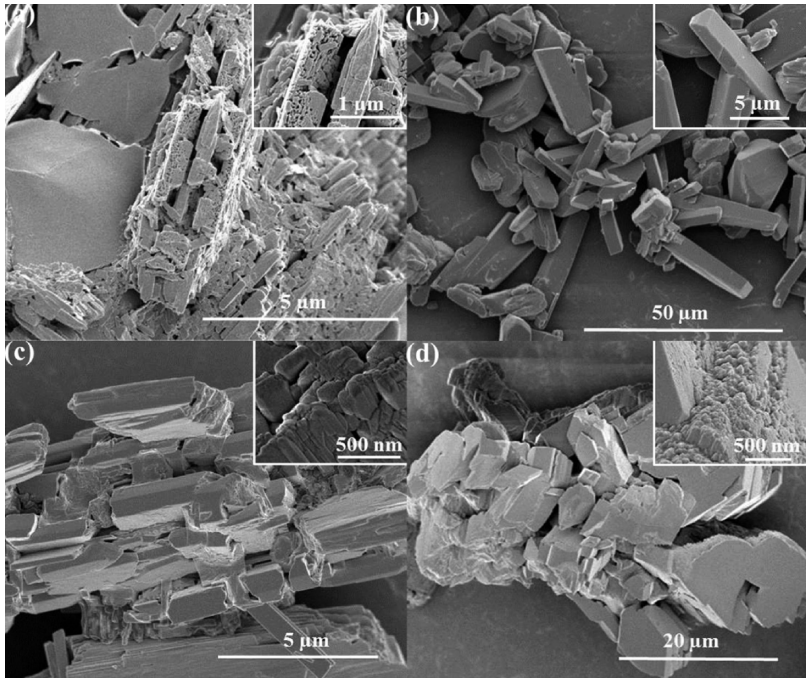

Figure 6. SEM images of as-synthesized Co-MOF microcrystals in the absence of a surfactant. (a) MW at 120 °C for 5 min, ramp time of 5 min; (b) MW at 160 °C for 5 min, ramp time of 30 min; (c) MW at 180 °C for 30 min, ramp time of 30 min; and (d) MW at 180 °C for 4 h, ramp time of 30 min. The images in the insets are close-up views of the Co-MOF microcrystals.

A series of experiments with different reaction times and temperatures were conducted to investigate the growth mechanism of the MOF microcrystals. Time-resolved investigations of MOF crystallization allowed the detection of crystalline intermediates under the individual reaction parameters. The shapes and morphologies of the MOF structures were monitored using SEM. The material was also characterized via thermogravimetric analysis (TG-DTA) and nitrogen sorption. To determine the effect of the surfactant on the shape and size of the product, contrasting experiments were conducted in both the absence and presence of the various surfactants. The SEM images in Figure 2 show the morphology of as-synthesized Co-MOF microcrystals obtained at 120 °C using a 5-min ramp time with and without the three surfactants and clearly reveal that three different shapes exist for the Co-MOF microcrystals. Figure 2 indicates that Co-MOF

dx.doi.org/10.1021/sc300036p | ACS Sustainable Chem. Eng. 2013, 1, 66−74

synthesized without a surfactant (no template) had a spindle-like microrod crystalline structure, whereas small crystal flakes (nanosheets/nanoplates) formed when the Co-MOF was prepared using CTAB. Nanosheets with relatively consistent sizes were observed when SDS was used as the surfactant. Nanorod-like shapes formed for the Co-MOF samples prepared in the presence of the P123 surfactant.

A detailed study was conducted to determine the effects of the template, reaction temperature, and time on the size, shape, and morphology of MOF microcrystals. The surfactants had a pronounced effect on the size and morphology of the materials. The surface layers of the crystals were found to incorporate the surfactants, provided that there was a degree of complementarity between the charge and size of the guest ions and interstices in the structure of the crystal boundary layers. Figure 3 shows as-synthesized Co-MOF microcrystals prepared using CTAB as the surfactant. The addition of the CTAB surfactant created distinctive differences in the size and morphology of the products. The figure clearly indicates that layer-by-layer growth from small primary nanosheets to the final layered microrods occurred as the temperature was increased from 120 to 160 °C and as the time increased from 5 to 30 min (Figure 3a and b). Further increases of the reaction temperature and time to 180 °C and 30 min, respectively, led to the continuous growth of the microcrystals (Figure 3c and d).

Scanning electron microscopy (SEM) images of the as-synthesized Co-MOF microcrystals obtained using SDS as a template are shown in Figure 4. This figure shows the 3D growth process of the primary nanosheets/nanoplates into larger multilayered microcubes after the temperature was increased from 120 to 160 °C and the time was increased from 5 to 30 min (Figure 4a and b). A further increase in the reaction temperature to 180 °C and reaction time to 30 min led to the continued growth of the microcubes into larger Co-MOF microcrystals. This finding suggests that relatively large Co-MOF microcrystals may grow from aggregated nascent nanosheets and that the presence of SDS is crucial for forming Co-MOF microrods with a relatively uniform size and shape.

The polymeric P123 surfactant yielded aggregated nanorods. Figure 5 clearly shows the growth process of the primary nanothreads into the larger multilayered microcrystals. A closer inspection of these nanorods (Figure 5d) reveals that they are composed of a large number of layered nanorods that are both interconnected with each other and self-organized in three dimensions to form Co-MOF microcrystals.

To determine the role that the various surfactants play in the growth mechanism of the Co-MOF microcrystals into different shapes and morphologies, time and temperature dependency was evaluated without the use of a surfactant by increasing the temperature from 120 to 160 °C and the time from 5 to 30 min. SEM images (Figure 6a and b) suggest that the growth process begins with small rectangular nanorods and eventually forms micrometer-sized rods. Increasing the reaction temperature and time further to 180 °C and 30 min, respectively, led to the continuous growth of these microrods (Figure 6c). Increasing the time to 4 h did not increase the size of the microrods further (Figure 6d).

As shown in Figure 6, primarily large, irregular microcrystals in the size range of 5−10 μm were obtained without a surfactant. The addition of various surfactants resulted in distinct variations in the size and morphology of the products. This finding clearly suggests that relatively large MOF microcrystals may be grown from aggregated primary nanosheets. The presence of a surfactant template is crucial for forming nanorods/nanosheets with relatively uniform sizes and shapes.

Textural Properties of the MOF. The textural properties of as-synthesized Co, Cu, and In MOFs were investigated by N_2 adsorption−desorption analysis. The N_2 adsorption and desorption isotherms presented in Figure 7 show that more

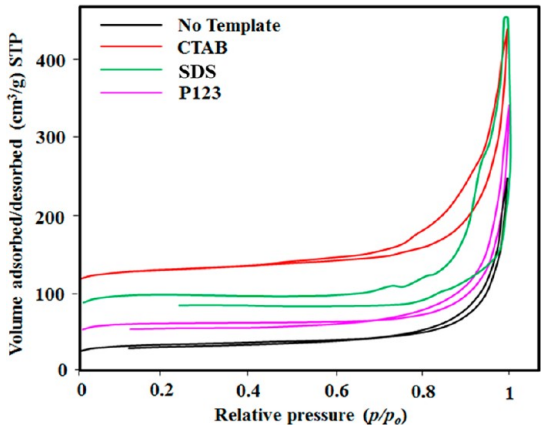

Figure 7. N_2 adsorption/desorption isotherms for the Cu-MOF microcrystals synthesized under microwave irradiation in the absence and presence of surfactants: (a) without surfactant, (b) CTAB, (c) SDS, and (d) P123. (MW at 120 °C for 0 min, ramp time of 5 min.)

N_2 gas was absorbed by Co-MOF samples prepared using the SDS template than those prepared using the CTAB and P123 templates. A comparatively low amount of N_2 gas was absorbed by Co-MOF samples prepared without any surfactant template (Figure 7). In addition, the larger hysteresis loops observed for the samples synthesized without a surfactant template indicate these samples had more pores with restricted access. All of the samples prepared without a template produced type-I isotherms, which are characteristic of microporous materials. The samples prepared using the CTAB, SDS, and P123 templates produced type IV isotherms, which are characteristic of mesoporous materials.

Table 1 (see the Supporting Information, Figures S3 and S11) shows the physical and textural properties of Co-MOF and In-MOF samples, and Table 2 (also see Supporting Information, Figure S6) shows the same properties for Cu-MOF samples. Table 1 shows a slight decrease in BET surface area for Co-MOF samples with increasing MW irradiation time (from 5 min to 4 h) and temperature (from 120 to 180 °C). This decrease may be the result of the increased size of the Co-MOF microcrystals.

Additionally, the effect of washing with ethanol on the textural properties of the Cu-MOF samples was also studied. Table 2 shows (see Supporting Information, Figure S6) the effect of varying the number of ethanol washes at 80 °C for 2 h. As the number of washes increased, the Brunauer−Emmett−Teller (BET) surface area and pore volume of the Cu-MOF samples increased. This increase in BET surface area and pore volume was associated with the removal of residual organic components (surfactant) from the pores of the MOF microcrystals. A similar trend was observed for Cu-MOF samples prepared using CTAB or P123 (Table 2).

The as-synthesized MOFs were also studied using powder X-ray diffraction (XRD) and thermogravimetric-differential analysis (TG-DTA). Figure 8 shows the XRD and TG-DTA

dx.doi.org/10.1021/sc300036p | ACS Sustainable Chem. Eng. 2013, 1, 66−74

Table 1. Textural Properties of Co-MOF and In-MOF Microcrystals Synthesized Using Different Microwave Heating Times and Temperatures

sample ID	BET surface area (m^2/g)	average pore diameter (Å)	BJH pore volumes (cm^3/g)
Cobalt-MOF (MW-120 °C for 0 min, ramp time of 5 min)			
no template	226	10.23	0.063
CTAB	293	11.26	0.078
SDS	317	11.59	0.072
P123	280	13.41	0.065
Cobalt-MOF (MW-120 °C for 5 min, ramp time of 5 min)			
no template	193	9.50	0.061
CTAB	281	11.04	0.073
SDS	279	11.49	0.069
P123	273	13.09	0.064
Cobalt-MOF (MW-160 °C for 5 min, ramp time of 30 min)			
no template	179	10.21	0.057
CTAB	276	12.10	0.069
SDS	271	12.39	0.065
P123	267	13.47	0.062
Cobalt-MOF (MW-180 °C for 30 min, ramp time of 30 min)			
no template	174	10.79	0.051
CTAB	267	12.51	0.063
SDS	264	13.82	0.059
P123	253	14.12	0.063
Cobalt-MOF (MW-180 °C, for 4h, ramp time of 30 min)			
no template	162	11.61	0.054
CTAB	257	13.10	0.068
SDS	249	14.33	0.079
P123	235	15.30	0.064
Indium-MOF (MW-120 °C for 4 h, ramp time of 30 min)			
no template	320	11.86	0.061
CTAB	432	12.10	0.071
SDS	530	11.39	0.065
P123	327	10.17	0.057

Table 2. Textural Properties of Cu-MOF Microcrystals Synthesized by Microwave Heating

sample ID	BET surface area (m^2/g)	average pore diameter (Å)	BJH pore volumes (cm^3/g)
Cu-MOF series (no template)			
1st wash	904	27.85	0.069
2nd wash	912	28.16	0.071
3rd wash	953	29.23	0.074
4th wash	977	29.67	0.075
5th wash	981	29.81	0.076
6th wash	984	29.83	0.078
(CTAB)			
1st wash	1098	33.10	0.058
2nd wash	1160	33.38	0.065
3rd wash	1243	33.57	0.076
4th wash	1336	33.74	0.079
5th wash	1339	33.76	0.086
6th wash	1344	33.79	0.087
(P123)			
1st wash	967	29.87	0.063
2nd wash	1098	30.05	0.064
3rd wash	1193	30.91	0.068
4th wash	1245	31.74	0.074
5th wash	1263	32.61	0.078
6th wash	1265	33.19	0.081

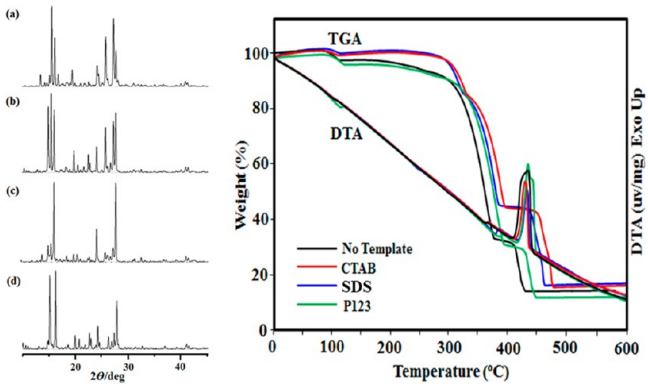

Figure 8. Powder X-ray diffraction patterns and TG-DTA curves for Co-MOFs synthesized with and without surfactants: (a) without surfactant, (b) CTAB, (c) SDS, and (d) P123. (MW at 120 °C for 0 min, ramp time of 5 min.)

patterns of Co-MOFs synthesized under microwave irradiation with and without the various surfactants using varying MW irradiation times and temperatures (Supporting Information, Figure S1). The main peak at 2θ = 9.86 corresponding to the Co-MOF microcrystal plane was observed in all samples, which confirms that Co-MOF crystals were successfully synthesized via microwave irradiation in the absence and presence of various surfactants. In addition, all of the samples were confirmed to be crystalline, and the relative crystallinity increased as the irradiation time increased (Supporting Information, Figure S1 (V)). A comparison of the powder X-ray diffraction results for Cu-MOFs to the standard XRD peaks of BTC (Supporting Information, Figure S7) indicated that the microcrystals obtained in the presence and absence of various surfactants were Cu-BTC MOFs.

The TG-DTA results for Co-MOF microcrystals synthesized using various surfactants and different MW irradiation times and temperatures were compared to those for samples prepared in the absence of any surfactant template. Figure 8 clearly demonstrates negligible weight loss in all of the Co-MOF samples at approximately 120 °C that arose from water molecules trapped in the micropores. There was no weight loss up to 325 °C for the samples prepared using CTAB and SDS. Both for samples prepared without a surfactant and for those prepared using P123, a steady, negligible weight loss was observed up to 350 °C. The sharp decrease in weight at 350 °C for all of the Co-MOF samples can be attributed to the thermal decomposition of the organic frameworks in the Co-MOF microcrystals. The sharp exothermic peaks in the DTA curves above 350 °C indicate the oxidation of the organic groups. These results were consistent for samples obtained using different MW irradiation times and temperatures (Supporting Information, Figure S2 (II–V)). Furthermore, we compared the TG-DTA results for the Cu-MOF and In-MOF samples synthesized in the absence of any surfactant to those for samples synthesized using the various surfactants. We observed a similar trend for all of the samples, regardless of the absence or presence of the various surfactants (Supporting Information, Figures S5 and S9).

Carbon Dioxide (CO_2) Capture. CO_2 is one of the major sources of the greenhouse effect, and significant efforts are currently directed to capturing CO_2 and preventing it from entering the atmosphere. Conventionally, such CO_2 sequestering has been accomplished via physical or chemical absorption

using aqueous basic solvents, such as amine solutions, with limited success because of the thermal instability of the solvents. Solid sorbents such as functionalized silica, zeolites, and carbon-based materials were then used because of their improved stability. In this regard, MOFs represent an important class of high-surface-area materials for CO_2 capture with high capture capacity and good thermal stability.[14−16,36] These properties led us to investigate as-synthesized Cu, Co, and In MOFs for the capture of CO_2.

Figure 9 shows the CO_2 adsorption/desorption performance of the as-synthesized MOFs up to a pressure of 10 bar at 25 °C

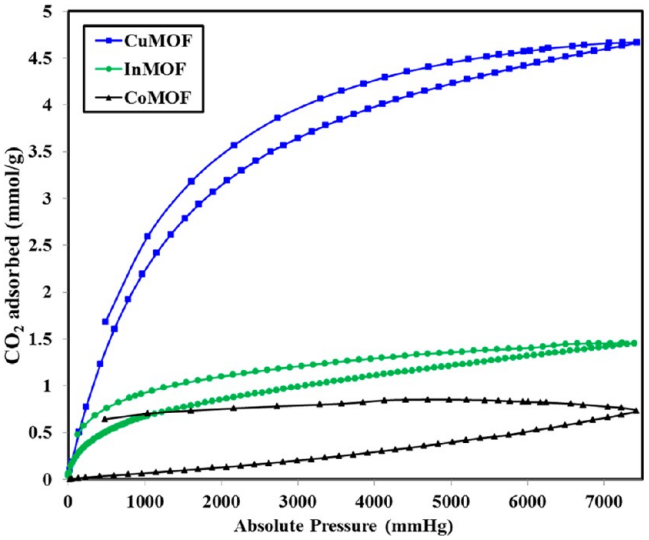

Figure 9. CO_2 adsorption isotherms of as-synthesized Co-, In-, and Cu-based MOFs.

using a volumetric technique. Cu-MOF showed better CO_2 capturing capacity than In- or Co-based MOFs. For all three of the MOFs, the CO_2 capture capacity increased with increasing pressure, which is indicative of the typical physisorption behavior for these materials.

MOFs were synthesized using an organic ligand (BTC) linked through metal joints (Cu, Co, and In) to form a porous framework. The specific metal used can significantly affect the adsorption capacity.[14,37] The nature of the interactions of CO_2 with the MOF depends on the bond between the metal center and the organic ligand, which dictates the electrostatic factor with the metal center having a partial positive charge. Increased exposure of these positive charges, even to the inner surface of the MOF, increases their interactions with CO_2, which increases the CO_2 capture capacity. To study this phenomenon, we tried to expose more of the metal center by repeatedly washing the MOF. Because the Cu-MOF samples exhibited the highest CO_2 capturing capacity of the studied materials, we chose this MOF to study the effects of repeated washing. Figure 10 shows the effect of washing on the CO_2 capture capacity for Cu-MOFs synthesized using different surfactants and without a surfactant. In all cases, the capture capacity increased for the first 3 washes. This number of washes also increased the surface area of the samples (Table 2). Thus, we concluded that, during these 3 washes, the removal of the surfactant (Supporting Information, Table S1) exposed an increasing number of cationic sites,[14,37] which resulted in increased CO_2 capture capacity. Similar observations were obtained for the Co- and In-MOFs (Figure 11).

CONCLUSION

In summary, we studied the effects of three surfactant templates (CTAB, SDS, and P123) on the size, shape, and morphology of three MOF (Co, Cu, and In) microcrystals. These surfactants strongly influenced the textural properties, morphology, and CO_2 capturing capacity of the as-synthesized MOF microcrystal samples. MOF microcrystals synthesized in the presence of a surfactant had highly porous nanostructures, whereas those synthesized without a surfactant had less porous nanostructures. We also studied the CO_2 capture capacity of the as-

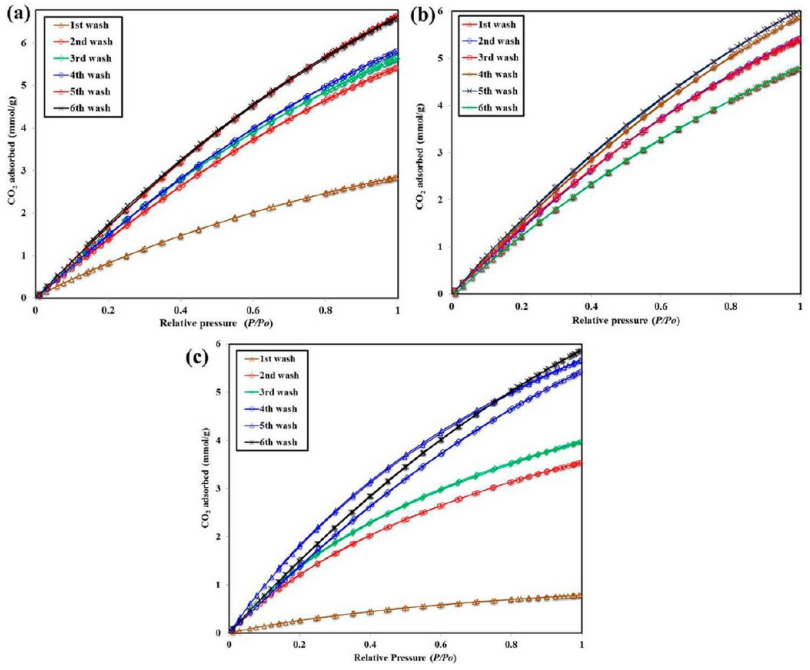

Figure 10. Effect of washing on the CO_2 adsorption isotherms for Cu-MOF (a) without using template, (b) using CTAB, and (c) using P123.

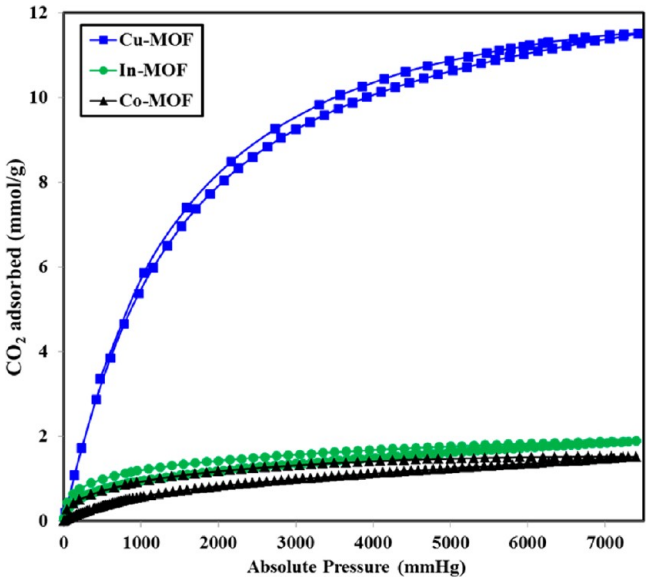

Figure 11. CO_2 adsorption isotherms of the as-synthesized Co-, In-, and Cu-based MOFs after 3 washes.

synthesized MOF microcrystals. Of the synthesized materials, the Cu-MOF samples exhibited the highest CO_2 capture capacity.

■ ASSOCIATED CONTENT

Supporting Information

More detailed information about the synthesis and characterization of MOFs as noted in the text. This material is available free of charge via the Internet at http://pubs.acs.org.

■ AUTHOR INFORMATION

Corresponding Author

*E-mail: vivek.pol@kaust.edu.sa. Tel.: (+966) 2 808-0302. E-fax: (+966) 2 802-1253.

Notes

The authors declare no competing financial interest.

■ ACKNOWLEDGMENTS

We thank King Abdullah University of Science and Technology (KAUST) for their funding and support. We also thank Prof. Mohamed Eddaoudi for his lecture on MOFs, which inspired us to engage in this work.

■ REFERENCES

(1) Zhou, H.-C.; Long, J. R.; Yaghi., O. M. Introduction to metal−organic frameworks. *Chem. Rev.* **2012**, *112*, 673−674.
(2) Czaja, A. U.; Trukhan, N.; Müller, U. Industrial applications of metal−organic frameworks. *Chem. Soc. Rev.* **2009**, *38*, 1284−1293.
(3) Stock, R.; Biswas, S. Synthesis of metal−organic frameworks (MOFs): Routes to various MOF topologies, morphologies, and composites. *Chem. Rev.* **2012**, *112*, 933−969.
(4) Chae, H. K.; Siberio-Perez, D. Y.; Kim, J.; Go, Y.; Eddaoudi, M.; Matzger, A. J.; O'Keeffe, M.; Yaghi, O. M. A route to high surface area, porosity and inclusion of large molecules in crystals. *Nature* **2004**, *427*, 523−527.
(5) Tranchemontagne, D. J.; Ni, M. O. K. Z.; Yaghi, O. M. Reticular chemistry of metal−organic polyhedra. *Angew. Chem., Int. Ed.* **2008**, *47*, 5136−5147.
(6) O'Keeffe, M. Design of MOFs and intellectual content in reticular chemistry: A personal view. *Chem. Soc. Rev.* **2009**, *38*, 1215−1217.
(7) Furukawa, H.; Ko, N.; Go, Y. B.; Aratani, N.; Choi, S. B.; Choi, E.; Yazaydin, A. O.; Snurr, R. Q.; O'Keeffe, M.; Kim, J.; Yaghi, O. M. Ultra-high porosity in metal−organic frameworks. *Science* **2010**, *239*, 424−427.
(8) Horcajada, P.; Chalati, T.; Serre, C.; Gillet, B.; Sebrie, C.; Baati, T.; Eubank, J. F.; Heurtaux, D.; Clayette, P.; Kreuz, C.; Chang, J. S.; Hwang, Y. K.; Marsaud, V.; Bories, P. N.; Cynober, L.; Gil, S.; Ferey, G.; Couvreur, P.; Gref, R. Porous metal−organic-framework nanoscale carriers as a potential platform for drug delivery and imaging. *Nat. Mater.* **2010**, *9*, 172−177.
(9) Kuppler, R. J.; Timmons, D. J.; Fang, Q. R.; Li, J. R.; Makal, T. A.; Young, M. D.; Yuan, D.; Zhao, D.; Zhuang, W.; Zhou, H. C. Potential applications of metal-organic frameworks. *Coord. Chem. Rev.* **2009**, *253*, 3042−3066.
(10) Li, J.-R.; Sculley, J.; Zhou, H.-C. Metal−organic frameworks for separations. *Chem. Rev.* **2012**, *112*, 869−932.
(11) Lee, J.-Y.; Farha, O. K.; Roberts, J.; Scheidt, K. A.; Nguyen, S. T.; Hupp, J. T. Metal−organic framework materials as catalysts. *Chem. Soc. Rev.* **2009**, *38*, 1450−1459.
(12) Huxford, R. C.; Rocca, J. D.; Lin, W. Metal−organic frameworks as potential drug carriers. *Curr. Opin. Chem. Biol.* **2010**, *14*, 262−268.
(13) Horcajada, P.; Serre, C.; Maurin, G.; Ramsahye, N. A.; Balas, F.; Vallet-Regí, M.; Taulelle, M.; F.; Férey, G. Flexible porous metal−organic frameworks for a controlled drug delivery. *J. Am. Chem. Soc.* **2008**, *130*, 6774−6780.
(14) Sumida, K.; Rogow, D. L.; Mason, J. A.; McDonald, T. M.; Bloch, E. D.; Herm, Z. R.; Bae, T.-H.; Long., J. F. Carbon dioxide capture in metal−organic frameworks. *Chem. Rev.* **2012**, *112*, 724−781.
(15) Li, J.-R.; Kuppler, R. J.; Zhou, H.-C. Selective gas adsorption and separation in metal−organic frameworks. *Chem. Soc. Rev.* **2009**, *38*, 1477−1504.
(16) Luebke, R.; Eubank, J. F.; Cairns, A. J.; Belmabkhout, Y.; Wojtasb, L.; Eddaoudi, M. The unique rht-MOF platform, ideal for pinpointing the functionalization and CO_2 adsorption relationship. *Chem. Commun.* **2012**, *48*, 1455−1457.
(17) Ozin, G. A., Arsenault, A. C., Cademartiri, L., Eds. *Nanochemistry: A chemical approach to nanomaterials*, 2nd ed; Royal Society of Chemistry: Cambridge, U.K., 2008.
(18) Cao, G., Wang, Y., Eds. *Nanostructures and nanomaterials*, 2nd ed.; World Scientific Publishing: 2011.
(19) Sun, L.; Li, J.; Park, J.; Zhou, H. Cooperative template-directed assembly of mesoporous metal−organic frameworks. *J. Am. Chem. Soc.* **2012**, *134*, 126−129.
(20) Pang, M.; Cairns, A. J.; Yunling Liu, Y.; Belmabkhout, Y.; Zeng, H. C.; Eddaoudi, M. Highly monodisperse M^{III}-based soc-MOFs (M = In and Ga) with cubic and truncated cubic morphologies. *J. Am. Chem. Soc.* **2012**, *134*, 13176−13179.
(21) Hu, L.; Zhang, P.; Chen, Q.; Zhong, H.; Hu, X.; Zheng, X.; Wang, Y.; Yang, N. Morphology-controllable synthesis of metal organic framework $Cd_3[Co(CN)_6]_2{\cdot}nH_2O$ nanostructures for hydrogen storage applications. *Cryst. Growth Des.* **2012**, *12*, 2257−2264.
(22) Huang, L.; Wang, H.; Chen, J.; Wang, Z.; Sun, J.; Zhao, D.; Yan, Y. Synthesis, morphology control, and properties of porous metal−organic coordination polymers. *Microporous Mesoporous Mater.* **2003**, *58*, 105−114.
(23) Li, Y. S.; Bux, H.; Feldhoff, A.; Li, G. L.; Yang, W. S.; Caro, J. Controllable synthesis of metal−organic frameworks: From MOF nanorods to oriented MOF membranes. *Adv. Mater.* **2010**, *22*, 3322−3326.
(24) Spokoyny, A. M.; Kim, D.; Sumrein, A.; Mirkin, C. A. Infinite coordination polymer nano- and microparticle structures. *Chem. Soc. Rev.* **2009**, *38*, 1218−1227.
(25) Liu, K.; Zheng, Y.; Jia, G.; Yang, M.; Huangab, Y.; You, H. Facile synthesis of hierarchically superstructured praseodymium benzene-tricarboxylate with controllable morphologies. *CrystEngComm* **2011**, *13*, 452−458.
(26) Hao, X.-R.; Wang, X.-L.; Shao, K.-Z.; Yang, G.-S.; Su, Z.-M.; Yuan, G. Remarkable solvent-size effects in constructing novel porous

1,3,5-benzenetricarboxylate metal−organic frameworks. *CrystEngComm* **2012**, *14*, 5596−5603.
(27) Polshettiwar, V.; Baruwati, B.; Varma, R. S. Self-assembly of metal oxides into 3D nano-structures: Synthesis and nano-catalysis. *ACS Nano* **2009**, *3*, 728−736.
(28) Polshettiwar, V.; Cha, D.; Zhang, X.; Basset, J. M. High surface area silica nanospheres (KCC-1) with fibrous morphology. *Angew. Chem., Int. Ed.* **2010**, *49*, 9652−9656.
(29) Fihri, A.; Sougrat, R.; Rakhi, R. B.; Rahal, R.; Cha, D.; Hedhili, M.; Bouhrara, M.; Alshareef, H. N.; Polshettiwar, V. Nano-roses of nickel oxides: Synthesis, electron tomography study, and application in co oxidation and energy storage. *ChemSusChem* **2012**, *5*, 1241−1248.
(30) Fihri, A.; Bouhrara, M.; Patil, U.; Cha, D.; Saih, Y.; Polshettiwar, V. Fibrous nano-silica supported ruthenium (KCC-1/Ru): A sustainable catalyst for the hydrogenolysis of alkanes with good catalytic activity and lifetime. *ACS Catal.* **2012**, *2*, 1425−1431.
(31) Rahal, R.; Wankhade, A.; Cha, D.; Fihri, A.; Ould-Chikh, S.; Patil, U.; Polshettiwar, V Synthesis of hierarchical anatase TiO_2 nanostructures with tunable morphology and enhanced photocatalytic activity. *RSC Adv.* **2012**, *2*, 7048−7052.
(32) Patil, U.; Fihri, A.; Emwas, A. H.; Polshettiwar, V. Silicon oxynitrides of KCC-1, SBA-15 and MCM-41 for CO_2 capture with excellent stability and regenerability. *Chem. Sci.* **2012**, *3*, 2224−2229.
(33) Polshettiwar, V.; Nadaguada, M. N.; Varma, R. S. MW-assisted chemistry: A rapid and sustainable route for synthesis of organics-nanomaterials. *Aust. J. Chem.* **2009**, *62*, 16−26.
(34) Polshettiwar, V., Varma, R. S., Eds. *Aqueous microwave assisted chemistry: Synthesis and catalysis*; Green Chemistry Series; Royal Society of Chemistry, Thomas Graham House, Science Park: Cambridge, U.K., 2010.
(35) Baruwati, B.; Polshettiwar, V.; Varma, R. S. Microwave-assisted synthesis of nanomaterial's in aqueous media. In *Aqueous Microwave Chemistry*; Polshettiwar, V., Varma, R. S., Eds.; RSC Green Chemistry Book Series; RSC Publishing: Cambridge, U.K., 2010.
(36) Millward, A. R.; Yaghi, O. M. Metal−organic frameworks with exceptionally high capacity for storage of carbon dioxide at room temperature. *J. Am. Chem. Soc.* **2005**, *127*, 17998−17999.
(37) Aprea, P.; Caputo, D.; Gargiulo, N.; Iucolano, F.; Pepe, F. Modeling carbon dioxide adsorption on microporous substrates: Comparison between Cu-BTC metal−organic framework and 13X zeolitic molecular sieve. *J. Chem. Eng. Data* **2010**, *55*, 3655−3661.